Scaling Factors for Models of Currents in Benzenoids

by

Parminder Kaur
B.Tech. Lovely Professional University 2013

A Master's Project Submitted in Partial Fullfilment of the
Requirements for the Degree of

MASTER OF SCIENCE

in the Department of Computer Science

Scaling Factors for Models of Currents in Benzenoids

by

Parminder Kaur
B.Tech. Lovely Professional University 2013

Supervisory Committee

Dr. Wendy Myrvold (Department of Computer Science)

Supervisor

Dr. Frank Ruskey (Department of Computer Science)

Committee member

Abstract

Conjugated-circuit (CC) methods give purely graph theoretical empirical models for estimation of molecular ring currents. This project considers the question of how to scale CC models to give better reproduction of the quantum mechanical Hückel–London model, in order to combine the transparency of the CC approach with the physical interoperability of the Hückel–London method. Scaling is carried such that L_1-errors and L_∞-errors are minimised for families of linear polyacenes and zigzag fibonacenes.

Contents

List of Tables

List of Figures

Acknowledgements

This work has been encouraged and become possible under the guidance of Dr. Wendy Myrvold. Thank you Wendy, for consistently encourage me to do better. I would also like to thank Patrick Fowler for his feedback on project, it was helpful.

I would like to express my gratitude to my best friend Navpreet who unconditionally took care of me during this journey and help me in accomplishing the dream of my parents.

1 Introduction

Ring currents have been at the heart of quantum chemistry for many decades. Ring currents are circulations of electrons induced in unsaturated carbon frameworks on application of a perpendicular external magnetic field. The Huckel-London model uses an empirical model for the response of a molecular electron distribution to external magnetic fields to calculate the currents that flow in the bonds of unsaturated carbon frameworks. The calculations require specification of both the molecular graph and the positions in space of the carbon centres. Currents are usually reported as ratios of the derivative of current with respect to field to the same quantity calculated for a benzene molecule. Huckel-London currents are typically in qualitative agreement with the results of more sophisticated quantum-chemical calculations, but are computed much more cheaply. This paper considers the Hückel–London current model [13] and several models based on conjugated-circuits; the model due to Randić [12], the model due to Ciesielski et. al. [5], the model due to Mandado [9] and the Two-term and the Adjusted Two-term models due to Myrvold and Fowler. The goal of our research is to find an approach for scaling conjugated-circuit models so that they provide approximations to Hückel–London currents.

We are considering two families of benzenoids, *linear polyacenes* which are polycyclic aromatic hydrocarbons consisting of linearly fused benzene rings. The smaller molecules (benzene, naphthalene, anthracene, tetracene,....) are shown in Figure 1. *Zigzag fibonacenes* (Figure 2) consist of chains of hexagons with a zigzag shape such that no straight segment is of length greater than two. There can be a number of ways zigzags can be plotted, our research considers only the ones which follow the pattern such that the ladder goes up as shown in Figure 2.

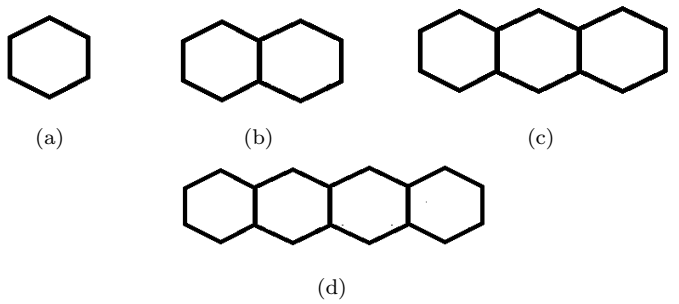

Figure 1: Linear polyacenes.

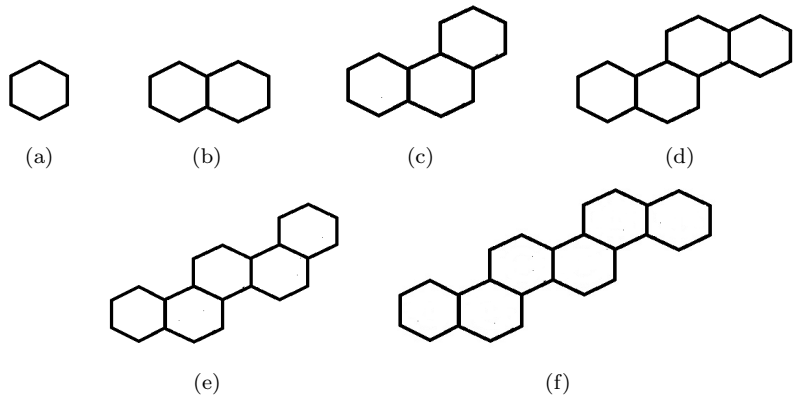

Figure 2: Zigzag fibonacenes.

The objective is to find an optimal value of a constant s which could be used to scale the Randić, Ciesielski et. al., Mandado, Two-term and Adjusted Two-term to the Hückel–London current model for linear polyacenes and zigzag fibonacenes. To achieve this, we use the mathematical optimization technique known as *linear programming*. Dantzig's Simplex algorithm [4] is used to extract optimal scaling factors for the different current models.

2 Background

2.1 Basic Graph Theory Definitions

This paper takes definitions from West's book [14]. An *undirected graph* G with n vertices and m edges consists of a *vertex set* $V(G) = \{ v_1, v_2...., v_n \}$ and an *edge set* $E(G) = \{e_1, e_2, ..., e_m\}$, where each edge corresponds to an unordered pair of vertices. The notation (u, v) is used for an edge between vertex u and vertex v. A *simple directed graph* or *digraph* G consists of a vertex set $V(G)$ and an arc set $E(G)$, where each arc corresponds to an ordered pair of vertices. We write $(u, v) \in E(G)$, if there is an arc from u to v. A *weighted directed graph* is a directed graph with weights assigned to its edges.

A cycle C is a graph with n vertices connected in a closed chain such that the number of vertices in C equals the number of edges, and every vertex has degree two. If G is a graph, then the subgraph induced by $S \subseteq V(G)$ is the graph H where $V(H) = S$ and $E(H) = \{(u, v) : (u, v) \in E(G)$ and $u, v \in S\}$.

A *matching* in an undirected graph G is a set of pairwise disjoint edges. The vertices belonging to the edges of a matching are *saturated* by the matching; the others are *unsaturated*. if a matching saturates every vertex of G, then it is a *perfect matching* or *complete matching*. In Chemistry, perfect matchings are called *Kekulé structures*. The number of perfect matchings of a graph G is denoted by $m(G)$. For all conjugated-circuit models for currents, $m(G)$ is assumed to be equal to one for a graph with no vertices.

A graph is *planar* if it can be drawn in the plane in such a way that none of its edges cross each other. If G is a planar graph, then any plane drawing of G divides the plane into regions, called *faces*. The graphs that correspond to *benzenoids* that are considered in this paper are planar graphs with no cut vertices, the vertices have degree two or three and all the internal faces are of size six, and also vertices not on the external face have degree three.

Given a molecular graph G, a current in G is represented by a weighted directed graph H such that $V(G) = V(H)$ and if G has edge (u, v) then H has

either arc (u, v) or (v, u). The weight on arc (u, v) represents the magnitude of the current from u to v.

Eigenvalues are a special set of scalars associated with a linear system of equations (i.e., a matrix equation) that are sometimes also known as characteristic roots. For a square matrix A of order n, the number λ is an eigenvalue if and only if there exists a non-zero vector x such that

$$Ax = \lambda x.$$

Using the matrix multiplication properties, we obtain

$$\Big(A - \lambda I_n\Big)x = 0.$$

The equation has a non trivial solution if

$$det\Big(A - \lambda I_n\Big) = 0.$$

The characteristic polynomial of a graph is the characteristic polynomial of its adjacency matrix. If the eigenvalues of the adjacency matrix for G are $\lambda_1, \lambda_2, \lambda_3, ..., \lambda_n$ then the characteristic polynomial for G can be written as:

$$(\lambda - \lambda_1)(\lambda - \lambda_2).....(\lambda - \lambda_n).$$

The characteristic polynomial of G with n vertices is given by:

$$\sum_{i=0}^{n} g_i \lambda^i.$$

Or equivalently, it can be written as:

$$g_0 + g_1\lambda^1 + g_2\lambda^2 + ... + g_n\lambda^n$$

where g_0, g_1, g_2, $g_3 ... g_n$ are coefficients of characteristic polynomial.

2.2 Conjugated-Circuits

In graph theory terms, a cycle C is a *conjugated-circuit* in a molecular graph G if both C and $G - C$ have a perfect matching [6].

2.3 Error between two current models

In a graph with arc (u, v), a current of magnitude $c_{u,v}$ from u to v is mathematically equivalent to a current of magnitude -$c_{v,u}$ from v to u. Figure 3 shows some equivalent currents. The *net current* on (u, v) is $c_{u,v}$ - $c_{v,u}$. The net current can be negative (see Figure 4).

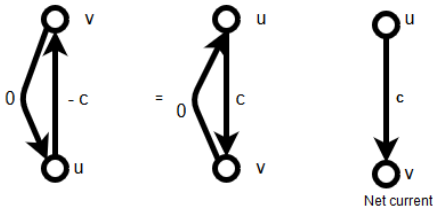

Figure 3: Some equivalent currents.

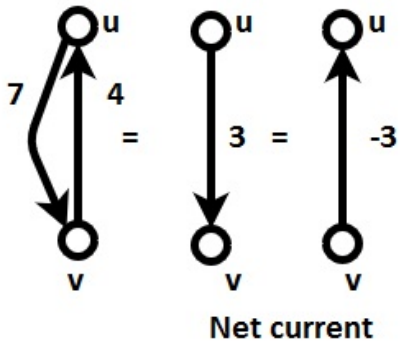

Figure 4: Examples of currents.

For two models A and B, let $c^A_{u,v}$ be the current on arc (u, v) for model A and let $c^B_{u,v}$ be the current for model B. The *difference* A-B of these two currents has current $c^A_{u,v}$ - $c^B_{u,v}$ on arc (u,v). The *magnitude of the difference* on arc (u,v) is defined to be $\mid c^A_{u,v} - c^B_{v,u} \mid$ and the direction is from u to v if $c_{u,v} > \ c_{v,u}$ and the direction is from v to u if $c_{v,u} > \ c_{u,v}$. For a current of zero value, an arbitrary direction is assigned. Current values c_1 and c_2 on a graph G are shown in Figures 5 and 6, respectively. Figure 7 shows the current difference c_1

- c_2.

In conjugated-circuit models, the computed current is the sum of contributions from all the conjugated-circuits. For all current models, the direction of the current contribution that corresponds to a cycle C is always the same. If C is a $4n$-cycle, the current is clockwise and if C is $(4n + 2)$- cycle, the current is counterclockwise. This reflects the chemical and physical distinction between anti-aromatic and aromatic carbon monocycles, where the induced current flows in the diamagnetic sense for the aromatic system, and in the opposite paramagnetic sense for the anti-aromatic system. However conjugated-circuit currents are weighted differently for the different models. After summing the conjugated-circuit currents, because of different weighting schemes, one model can have positive current from u to v where another model may have positive current going from v to u.

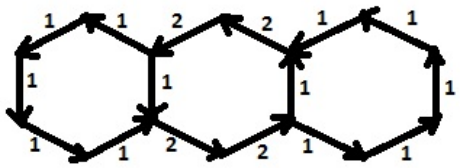

Figure 5: Current c_1 on G.

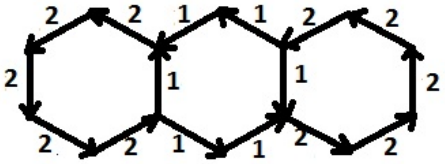

Figure 6: Current c_2 on G.

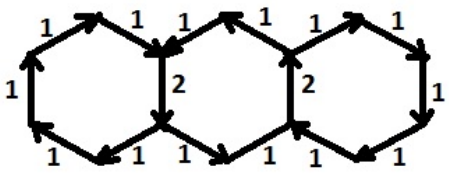

Figure 7: The current difference $c_1 - c_2$.

2.4 Current Models

As mentioned in introduction we are considering conjugated-circuit models; the Randić model, the Ciesielski et. al. model and the Mandado model. This section provides details on their definitions.

2.4.1 The model proposed by Randić

To compute an approximation for the current, Randić [12] considers all ordered pairs of perfect matchings. For every cycle that results, there is assignment of one unit of current going clockwise if the cycle is a $4n$-cycle and counterclockwise if it is a $(4n + 2)$-cycle. Then, all cycle currents are summed up and scaled by dividing by $m(G)(m(G) - 1)$.

To illustrate the calculation of the Randić current, we have taken an example of a 3-hexagon zigzag fibonacene. Figure 8 shows all matchings for this molecular graph.

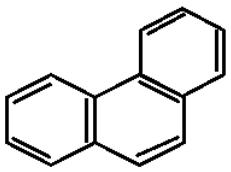

(a) Matching M_1.

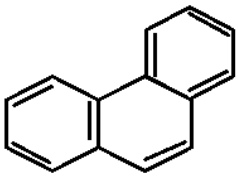

(b) Matching M_2.

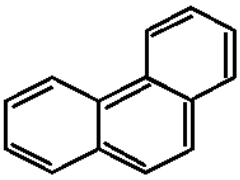

(c) Matching M_3.

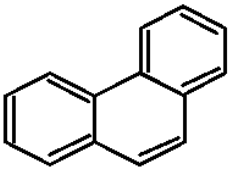

(d) Matching M_4.

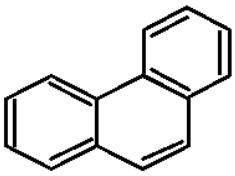

(e) Matching M_5.

Figure 8: Matchings for the 3-hexagon zigzag fibonacene.

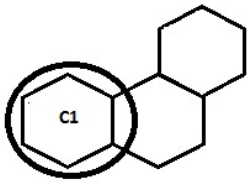

(a) Cycle C_1.

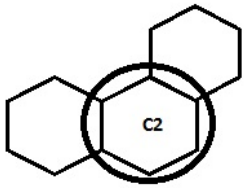

(b) Cycle C_2.

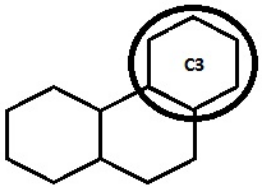

(c) Cycle C_3.

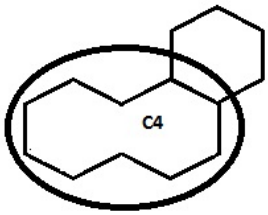

(d) Cycle C_4.

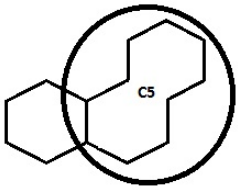

(e) Cycle C_5.

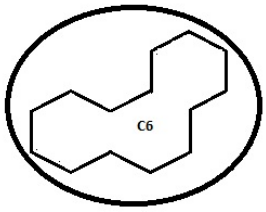

(f) Cycle C_6.

Figure 9: Cycles for the 3-hexagon zigzag fibonacene.

Figure 9 shows the six cycles C_1, C_2, C_3, C_4, C_5 and C_6 in the 3-hexagon zigzag fibonacecne. The matrix of matchings in Table 1 is formed by considering the ordered pairs of perfect matchings. The current on an edge e is the sum of these cycle currents for all cycles that include edge e arising by pairing perfect

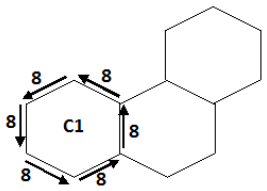

(a) Current for C_1.

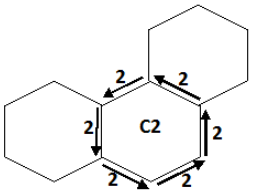

(b) Current for C_2.

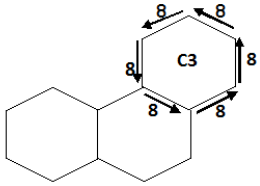

(c) Current for C_3.

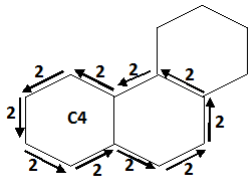

(d) Current for C_4.

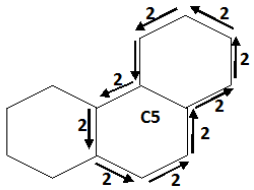

(e) Current for C_5.

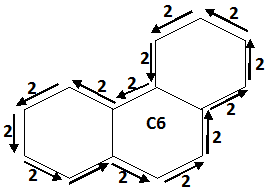

(f) Current for cycle C_6.

Figure 10: Randić current weights for each cycle in the 3-hexagon zigzag fibonacene found by vector addition of bond currents.

	M_1	M_2	M_3	M_4	M_5
M_1	$\times$	C_3	C_2	$C_1 + C_3$	C_1
M_2	C_3	$\times$	C_5	C_1	$C_1 + C_3$
M_3	C_2	C_5	$\times$	C_6	C_4
M_4	$C_1 + C_3$	C_1	C_6	$\times$	C_3
M_5	C_1	$C_1 + C_3$	C_4	C_3	$\times$

Table 1: Conjugated-circuits that result from each pair of matchings.

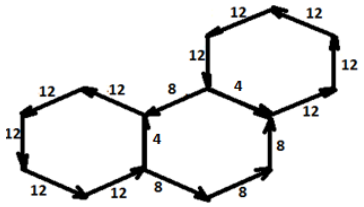

Figure 11: Sum of currents for all cycles on the 3-hexagon zigzag fibonacene, using the Randić current model.

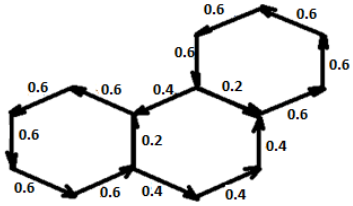

Figure 12: Final currents on the 3-hexagon zigzag fibonacene, using the Randić current model.

matchings. For example, cycle C_1 appears eight times in the matrix which results in a current weight of eight units on cycle C_1 and other cycles are also weighted similarly as shown in Figure 10. Figure 11 shows sum of currents on each cycle. Figure 12 shows the final current on the zigzag fibonacene obtained by adding the currents on each edge, and then scaling.

2.4.2 The model proposed by Ciesielski et. al.

The Ciesielski et. al. model [5] also considers ordered pairs of perfect matchings. The area of a cycle C in a benzenoid, $Area(C)$, is the number of hexagons inside C. Thus, all face areas are specified in terms of a standard hexagon. The Ciesielski et. al. model puts $Area(C)$ units of current on C for each pair of perfect matchings that includes C. For every cycle, there is assignment of $Area(C)$ units current going clockwise if the cycle is a $4n$-cycle and counterclockwise if it is a $(4n + 2)$-cycle.

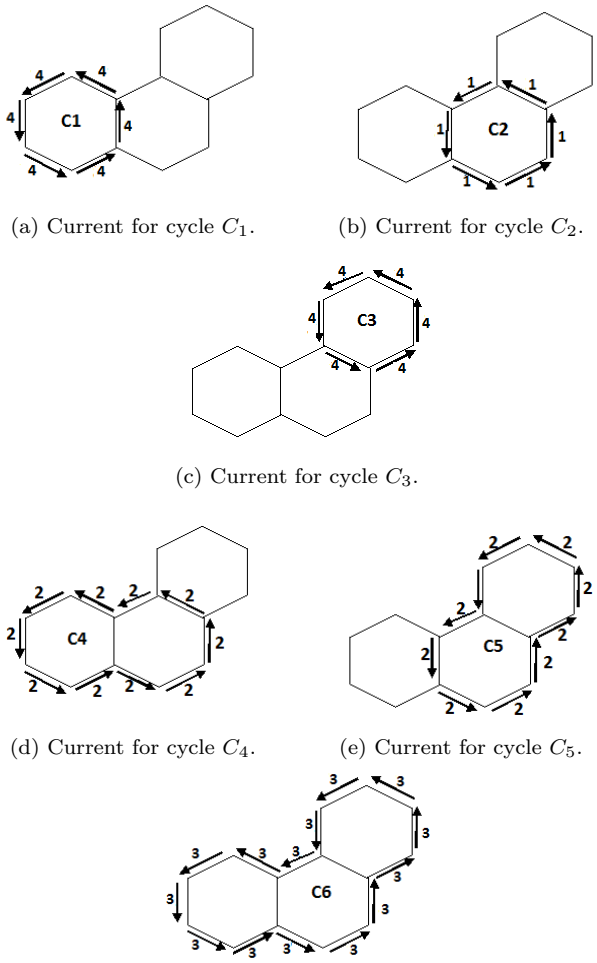

(a) Current for cycle C_1.

(b) Current for cycle C_2.

(c) Current for cycle C_3.

(d) Current for cycle C_4.

(e) Current for cycle C_5.

(f) Current for cycle C_6.

Figure 13: Current weights in the Ciesielski et. al. model on each cycle in a 3-hexagon zigzag fibonacene.

Figure 14 shows sum of currents on each cycle. The final current is the sum of these currents over all the ordered pairs of perfect matchings scaled by dividing by $m(G)(m(G)-1)$. The final current computed using the Ciesielski et. al. current model for a 3-hexagon zigzag fibonacene is shown in Figure 15.

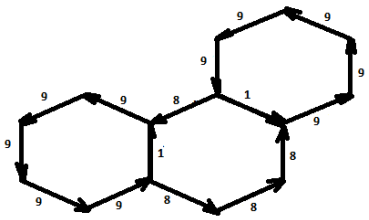

Figure 14: Sum of currents on each cycle of 3-hexagon zigzag fibonacene using the Ciesielski et. al. current model.

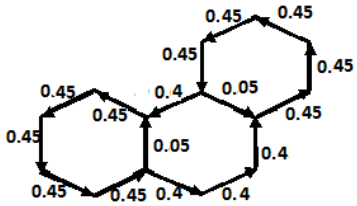

Figure 15: Final current on a 3-hexagon zigzag fibonacene using the Ciesielski et. al. current model.

2.4.3 The model proposed by Mandado

Mandado [9] considered all pairs of perfect matchings, as did Randić but discards the cases that have more than one cycle, see Table 2. For every cycle that results, $\frac{1}{Area(C)}$ units of currents is assigned to go clockwise if the cycle is a $4n$-cycle and counterclockwise if it is a $(4n+2)$-cycle. The $Area(C)$ is the number of hexagons inside C. Then, all cycle currents are summed up on edges in Figure 17 and are scaled by dividing by $m(G)$ as shown in Figure 18.

	M_1	M_2	M_3	M_4	M_5
M_1	$\times$	C_3	C_2	~~$C_1 + C_3$~~	C_1
M_2	C_3	$\times$	C_5	C_1	~~$C_1 + C_3$~~
M_3	C_2	C_5	$\times$	C_6	C_4
M_4	~~$C_1 + C_3$~~	C_1	C_6	$\times$	C_3
M_5	C_1	~~$C_1 + C_3$~~	C_4	C_3	$\times$

Table 2: Pairs of matchings that contribute to the Mandado current model

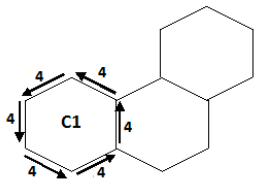

(a) Current for C_1.

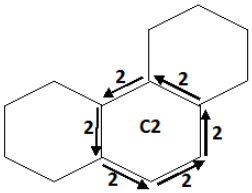

(b) Current for C_2.

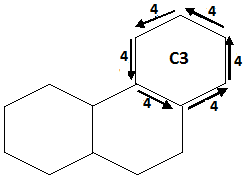

(c) Current for C_3.

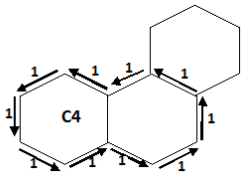

(d) Current for C_4.

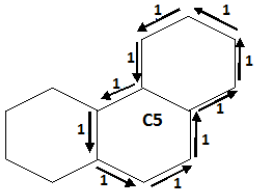

(e) Current for C_5.

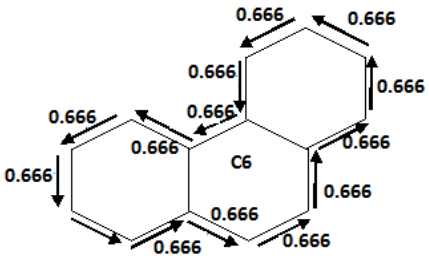

(f) Current for cycle C_6.

Figure 16: Mandado current weights on each cycle in the 3-hexagon zigzag fibonacene.

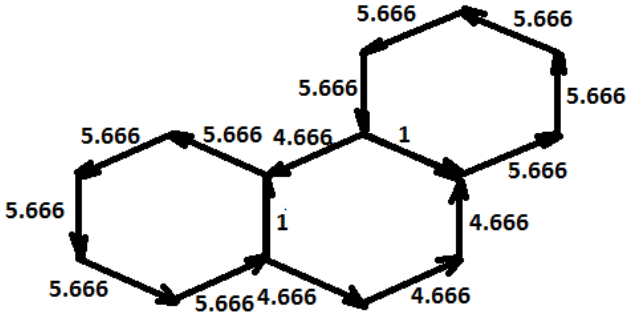

Figure 17: Sum of currents on each cycle of the 3-hexagon zigzag fibonacene, using the Mandado current model.

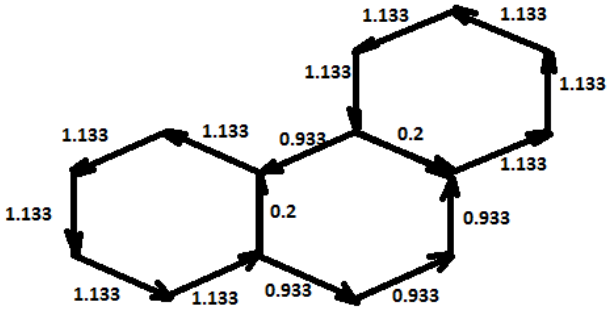

Figure 18: Final currents on the 3-hexagon zigzag fibonacene, using the Mandado current model.

2.5 Framework for Combinatorial models

Myrvold and Fowler [6] provided a combinatorial framework that encompasses the conjugated-circuit models of Randić [12], Ciesielski et. al. [5] and Mandado [9]. A cycle C in the undirected graph G corresponds to two directed cycles in the corresponding directed graph $\vec{G}$, one that is oriented clockwise and another that is oriented counterclockwise. The current is assigned to the clockwise directed cycle if C is a $4n$-cycle and to the counterclockwise directed cycle if C is a $(4n + 2)$-cycle. For the cycles that are not conjugated-circuits, the

contribution is zero.

The models use different formulas for the weight of a circuit current. The Randić, Ciesieleski et. al. and Mandado models put a weight on each conjugated-circuit which can be formalized in the following framework:

$$w(C) = \frac{1}{S} 2m(G-C)^p Area(C)^k \tag{1}$$

where the value of p is two for the Randić model and Ciesielski models and one for the Mandado model, the value of k is zero for the Randić model, one for the Ciesielski model and -1 for the Mandado model, and the value of S is equal to $m(G)(m(G)-1)$ for the Randić and Ciesielski models and $m(G)$ for the Mandado model. The value of $Area(C)$ is the number of hexagons inside C. Table 3 shows the models and their conjugated circuit current contributions.

Model	Conjugated circuit current
Randić	$2[m(G-C)^2]$
Ciesielski et. al.	$2[m(G-C)^2]Area(C)$
Mandado	$\frac{2[m(G-C)]}{Area(C)}$

Table 3: Conjugated circuit models and their currents

If $G-C$ has $m(G-C)$ perfect matchings, considering the same example of a 3-hexagon zigzag fibonacene as in Figure 8, we will again calculate Randić currents using equation (1). For every cycle that results, we compute the number of matchings for $G-C$ where C can be any cycle C_1, C_2, C_3, C_4, C_5 or C_6 as shown in Figure 19. We obtain the values of unscaled current on C shown in Table 4.

Cycle C	$m(G-C)$	Randić model	Ciesielski et.al. model	Mandado model
C_1	2	8	8	4
C_2	1	2	2	2
C_3	2	8	8	4
C_4	1	2	4	1
C_5	1	2	4	1
C_6	1	2	6	2/3

Table 4: Unscaled current for each cycle for the Randić, Ciesielski et.al. and Mandado models

The Randić weights computed in Table 4 are the same as shown in Figure 10. Then, all cycle currents are summed up and final current is shown in Figure 12 by scaling by multiplying by $\frac{1}{m(G)(m(G)-1)}$, where $m(G) = 5$, is the number of matchings of the graph G.

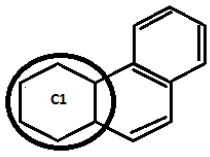

(a) One perfect matching for G-C_1.

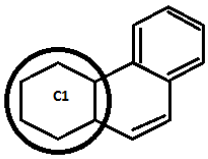

(b) A second perfect matching for G-C_1.

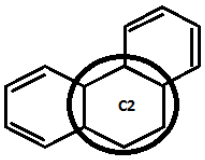

(c) A unique perfect matching for G-C_2.

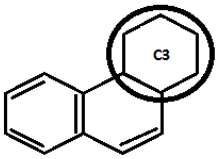

(d) One perfect matching for G-C_3.

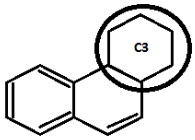

(e) A second perfect matching for G-C_3.

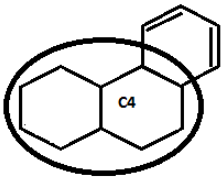

(f) A unique perfect matching for G-C_4.

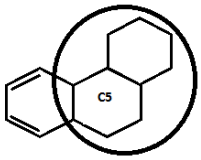

(g) A unique perfect matching for G-C_5.

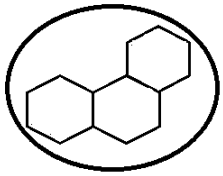

(h) A unique perfect matching for G-C_6.

Figure 19: Perfect matchings for $G - C$ graphs.

2.5.1 Two-term and Adjusted Two-term models proposed by Myrvold and Fowler

The Two-term and Adjusted Two-term models [11] were inspired by Aihara's formulas [1], [2], [8] for Hückel–London currents. These models are not published yet.

As mentioned in Section 2.1, the characteristic polynomial of a graph can be written as:

$$g_0\lambda^0 + g_1\lambda^1 + g_2\lambda^2 + ... + g_n\lambda^n$$

where $g_0, g_1, g_2.....g_n$ are the coefficients of the characteristic polynomial. For

benzenoids, g_0 (the constant term) is equal to $(-1)^{n/2}\ m(G)\ m(G)$. Hence, g_0 is always non-zero for graphs with perfect matchings. Let r_0 be the minimum value of i such that $g_i \neq 0$.

The weight for the current for a Circuit C is computed as shown in Table 5.

Two-term model	$w(C) = 2 * Area(C) * [c_{r_0}/g_{r_0} + c_{r_0+2}/g_{r_0+2}]$
Adjusted Two-term model	$w(C) = 2 * Area(C) * [c_{r_0}/g_{r_0} + 4 * c_{r_0+2}/g_{r_0+2}]$

Table 5: Two new models proposed by Myrvold and Fowler

If C is a $(4n)$-Cycle, $w(C)$ will be positive and $w(C)$ units are assigned to C in the clockwise direction. If C is a $(4n+2)$-cycle, $w(C)$ will be less than or equal to zero and $\mid w(C) \mid$ units are assigned to C in the counterclockwise direction. One approach to find eigenvalues and hence also characteristic polynomials is to use Jacobi's method [10].

2.5.2 Examples of the Two-term and Adjusted Two-term models

Consider the 3-hexagon linear polyacene with cycles C_1, C_2, C_3, C_4, C_5 and C_6 as shown in Figure 20. The coefficients of the characteristic polynomial of G are given in Table 6. The coefficients of the characteristic polynomial for each $G-C$ graph are given in Table 7. Tables 8 and 9 shows the contribution of current for each cycle and finally Figures 21 and 22 show final currents corresponding to the Two-term and Adjusted Two-term models by summing up contribution of each cycle over every edge.

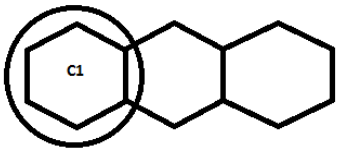

(a) Cycle C_1.

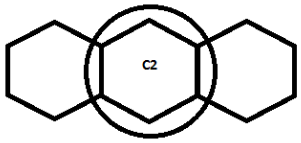

(b) Cycle C_2.

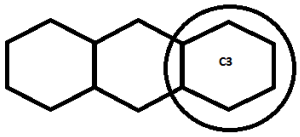

(c) Cycle C_3.

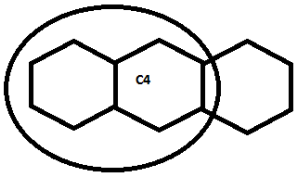

(d) Cycle C_4.

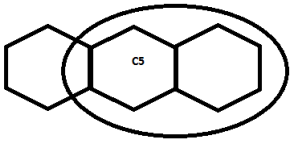

(e) Cycle C_5.

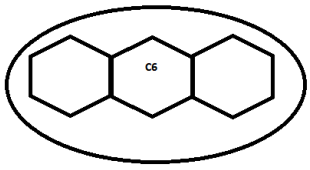

(f) Cycle C_6.

Figure 20: Cycles in 3-hexagon linear polyacenes.

g_0	g_1	g_2	g_3	g_4	g_5	g_6	g_7
-16	0	148	0	-392	0	473	0
g_8	g_9	g_{10}	g_{11}	g_{12}	g_{13}	g_{14}	
-296	0	98	0	-16	-0	1	

Table 6: The g_i values for the 3-hexagon linear polyacene.

Graph $\downarrow c_i \rightarrow$	c_0	c_1	c_2	c_3	c_4	c_5	c_6	c_7	c_8
C_1	1	0	-13	0	18	0	-8	0	1
C_2	1	0	-6	0	11	0	-6	0	1
C_3	1	0	-13	0	18	0	-8	0	1
C_4	1	0	-3	0	1				
C_5	1	0	-3	0	1				
C_6	1								

Table 7: The c_i values for the $G - C$ graphs for cycles C_1 to C_6.

Graph	$w(C) = 2 * Area(C) * [c_{r_0}/g_{r_0} + c_{r_0+2}/g_{r_0+2}]$	computed w(C)
C_1	$2 * 1 * [(1/-16) + (-13/148)]$	-0.3006757
C_2	$2 * 1 * [(1/-16) + (-6/148)]$	-0.2060811
C_3	$2 * 1 * [(1/-16) + (-13/148)]$	-0.3006757
C_4	$2 * 2 * [(1/-16) + (-3/148)]$	-0.3310811
C_5	$2 * 2 * [(1/-16) + (-3/148)]$	-0.3310811
C_6	$2 * 3 * [(1/-16) + (0/148)]$	-0.375

Table 8: The current contributions for each cycle for the Two-term model.

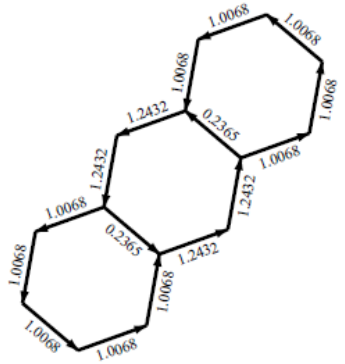

Figure 21: The Two-term model currents for the 3-hexagon linear polyacene.

Graph	$w(C) = 2 * Area(C) * [c_{r_0}/g_{r_0} + 4 * c_{r_0+2}/g_{r_0+2}]$	computed w(C)
C_1	2* 1 * [(1 / -16) + 4 * (-13 / 148)]	0.8277027
C_2	2* 1 * [(1 / -16) + 4 * (-6 / 148)]	0.4493243
C_3	2* 1 * [(1 / -16) + 4 * (-13 / 148)]	0.8277027
C_4	2* 2 * [(1 / -16) + 4 * (-3 / 148)]	0.5743243
C_5	2* 2 * [(1 / -16) + 4 * (-3 / 148)]	0.5743243
C_6	2* 3 * [(1 / -16) + 4 * (0 / 148)]	0.375

Table 9: The current contributions for each cycle for the 3-hexagon linear polyacene.

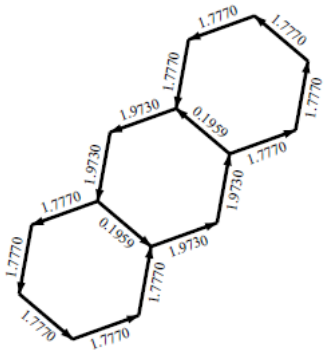

Figure 22: The Adjusted Two-term current for the 3-hexagon linear polyacene.

These two new models predict currents for molecules with no perfect matchings where all existing CC models give zero current for those molecules. The 13-vertex benzenoid shown in Figure 23 is example of such a molecule.

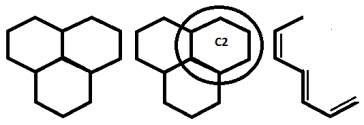

Figure 23: No perfect matching for $G - C_7$ graph.

This benzenoid has seven cycles C_1, C_2, C_3, ... C_7 as shown in Figure 24.

For i = 1,2, ...,7 , G–C_i has an odd number of vertices and hence $m(G$–$C_i)$ = 0. The Two-term model uses characteristic polynomials, the eigenvalues and the characteristic polynomials for $G - C$ for each Cycle C to determine current.

Using these terms in Two-term formula given in Table 5, the final current on the 13-vertex benzenoid is given in Figure 26. The resultant g_i values are shown in Table 10. Table 11 shows the resultant values of c_i. The current contribution for each cycle are given in Table 12 and the direction of current on each cycle is shown in Figure 25.

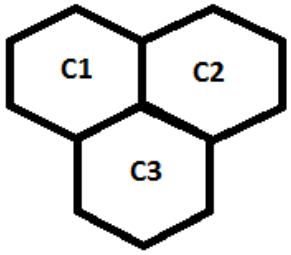

(a) Cycles C_1, C_2, C_3.

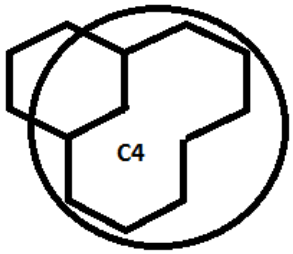

(b) Cycle C_4.

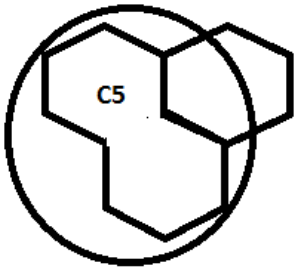

(c) Cycle C_5.

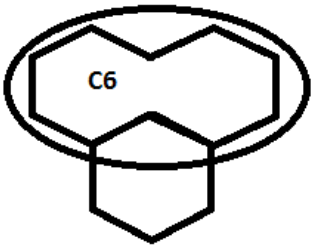

(d) Cycle C_6.

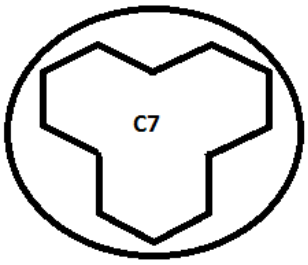

(e) Cycle C_7.

Figure 24: Cycles in a 13-vertex benzenoid.

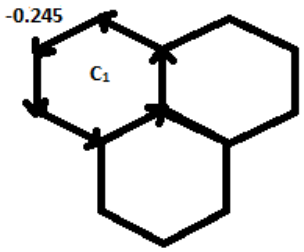

(a) Two-term current for Cycle C_1.

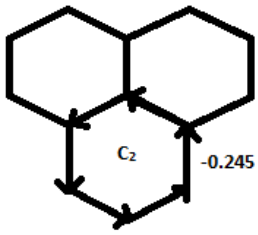

(b) Two-term current for Cycle C_2.

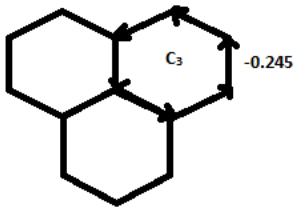

(c) Two-term current for Cycle C_3.

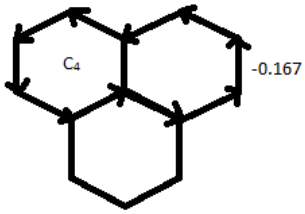

(d) Two-term current for Cycle C_4.

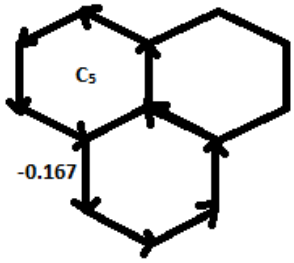

(e) Two-term current for Cycle C_5.

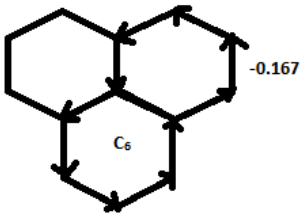

(f) Two-term current for Cycle C_6.

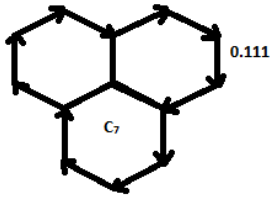

(g) Two-term current for Cycle C_7.

Figure 25: Two-term current for Cycles in 13-vertex benzenoid.

g_0	g_1	g_2	g_3	g_4	g_5	g_6	g_7
0	54	0	-207	0	309	0	-226
g_8	g_9	g_{10}	g_{11}	g_{12}	g_{13}		
0	84	0	-15	0	1		

Table 10: The g_i values for the 13-vertex benzenoid from Figure 20.

Graph $\downarrow$ c_i $\rightarrow$	c_0	c_1	c_2	c_3	c_4	c_5	c_6	c_7
$G - C_1$	0	-4	0	10	0	-6	0	1
$G - C_2$	0	-4	0	10	0	-6	0	1
$G - C_3$	0	-4	0	10	0	-6	0	1
$G - C_4$	0	-2	0	1				
$G - C_5$	0	-2	0	1				
$G - C_6$	0	-2	0	1				
$G - C_7$	0	1						

Table 11: The c_i values for the $G-C$ graphs for cycles C_1 to C_7 for the 13-vertex benzenoid.

Cycles	$w(C) = 2 * Area(C) * [c_{r_0}/g_{r_0} + c_{r_0+2}/g_{r_0+2}]$	computed w(C)
C_1, C_2, C_3	$2 * 1 * [(-4/54) + (10/-207)]$	-0.2447665
C_4, C_5, C_6	$2 * 2 * [(-2/54) + (1/-207)]$	-0.1674718
C_7	$2 * 3 * [(1/54) + (0/-207)]$	0.1111111

Table 12: The current contributions for each cycle for the Two-term model for the 13 vertex benzenoid.

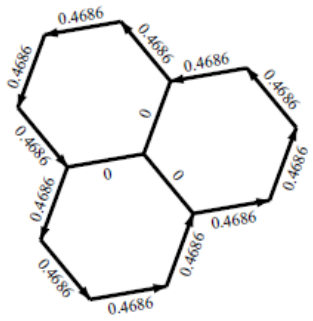

Figure 26: The Final Two-term current for 13-vertex benzenoid.

3 Scaling Current Models

Suppose $\vec{G}$ is a current graph. Scaling $\vec{G}$ by a constant s results in a new current such that for each arc (u, v) with the current $c_{u,v}$ in $\vec{G}$, the scaled current is s $c_{u,v}$. If the goal is to scale a current B to the best match a current A, then the error on edge (u, v) is equal to $\mid C_A(u, v) - C_B(u, v) \mid$. The L_1- error is defined to be the sum of the errors on each edge of the graph G. The L_∞- error is defined to be maximum of the errors on each edge of the graph G.

4 Finding Scaling factors using Linear Programming

Formally, a linear programming problem is the problem of maximizing (or minimizing) a linear function subject to a finite number of linear constraints. The standard form of a linear programming problem [4] is

Maximize $c^T x$
subject to
Ax $\leq$ b
x $\geq$ 0

where A is a n $\times$ m matrix of coefficients, c and b are vectors and x is the vector of variables to be found.

Suppose G_1 and G_2 are directed graphs with currents c^A and c^B flowing on an arc (u, v), computed by models A and B respectively. Let us assume that c^A is equal to the value of the current to match and c^B is the current we want to scale to get an optimal match to c^A. The next two sections present the linear programming problems used to scale c^B while minimizing the L_∞-error (section 4.1) and the L_1-error (section 4.2).

4.1 Minimizing L_∞-error

To minimize the L_∞-error while scaling model B to match model A, using the L_∞ approach:
The number of variables will be equal to two: an error r and a constant s which is the scaling factor. The direction of current is same for benzenoids considered in this paper so s is greater than zero or zero. The number of equations will be equal to twice number of edges of the graph.

The problem can be formulated as follows
Minimize r
subject to

for each edge (u, v) in the undirected graph G,
$r \geq | \, c^A_{u,v} - s \, c^B_{u,v} \, |$ and
$r, \, s \geq 0$.
The standard form of problem is:

Maximize $-r$
subject to:

for each edge (u, v) in the undirected graph G,
$-r - sc^B_{u,v} \leq -c^A_{u,v}$,
$-r + sc^B_{u,v} \leq c^A_{u,v}$, and

r, $s \geq 0$.

4.2 Minimizing L_1-error

To minimize the total absolute error while scaling model B to match model A by using the L_1 approach:
The edges of G are numbered as $e_1, e_2, e_3.....e_m$. For each edge e_i, there is a variable r_i that is the error for edge i. There is also the variable s (the scaling factor). The direction of current is same for benzenoids considered in this paper so s is greater than zero or zero. The number of variables will be equal to the number of edges of the graph plus one. The number of equations will be equal to twice the number of edges of the graph.
The problem can be formulated as follows:

Minimize $r_1 + r_2 + r_3 + \ldots + r_m$

subject to:

for each edge (u, v) in the undirected graph G,
$r_i \geq | c^A_{u,v} - s c^B_{u,v} |$ and
$r_1, r_2, r_3 \ldots, r_m$, $s \geq 0$.

The standard form for the L_1-norm for scaling current is:
Maximize -$(r_1 + r_2 + r_3 + \ldots + r_m)$

subject to:

for each edge (u, v) in the undirected graph G

$-r_i - s c^B_{u,v} \leq -c^A_{u,v}$,

$-r_i + s c^B_{u,v} \leq c^A_{u,v}$ and r, $s \geq 0$.

4.3 Example

Suppose G_1 and G_2 are directed graphs with currents c^A and c^B, computed using the Hückel–London model and the Mandado model respectively as shown in Figures 27 (a) and (b) respectively.

The optimal scaling factor for the L_1-norm is 1.183 and for the L_∞-norm is 1.097. For each scaling factor, we multiply the values of current generated by Mandado model (c^B) by the constant s (scaling factor) to get the scaled current ($s \times c^B$). Now, using the Hückel–London current, c^A and the scaled Mandado current sc^B, the difference is computed as shown in Figures 27(e) and 27(f) for the L_1-norm and L_∞-norm. The L_1-error is 0.605 and the L_∞-error is 0.079.

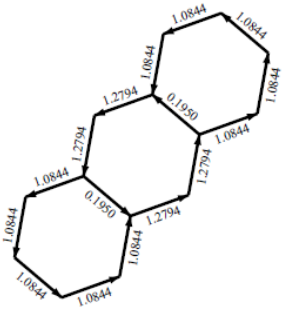

(a) Hückel–London current, c^A.

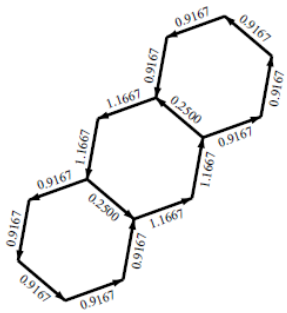

(b) Mandado current, c^B.

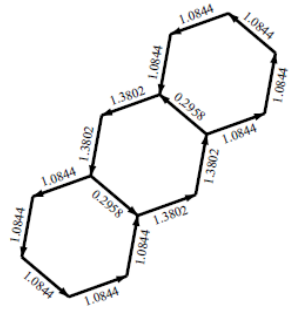

(c) Mandado current scaled by multiplying by 1.183 (optimal solution using the L_1-norm).

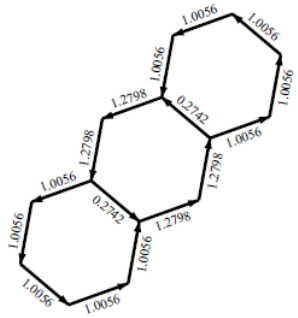

(d) Mandado current scaled by multiplying by 1.097 (optimal solution using the L_∞-norm).

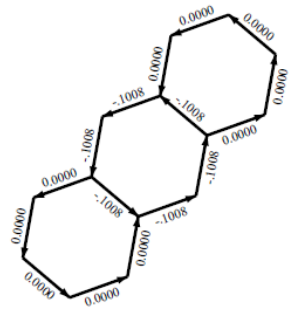

(e) The difference between Hückel–London current and scaled the Mandado current from (c).

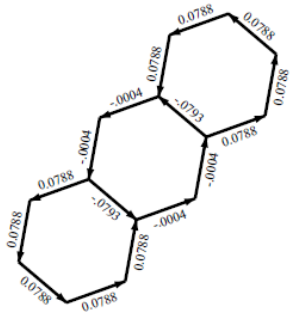

(f) The difference between Hückel–London current and scaled Mandado current from (d).

Figure 27: Scaling Mandado currents to Hückel–London currents.

5 Results

For the Mandado, Randić, Ciesielski et. al., Two-term and Adjusted Two-term models, we have calculated scaling factors for the linear polyacenes and zigzag fibonacenes using the L_∞ and L_1 approaches and the results are shown in Tables 13 and 16 respectively. The errors are shown in Tables 17-20. The cases which gave the best match to Hückel–London are highlighted in bold.

Number of hexagons → Model ↓	1	2	3	4	5	6	7	8	9
Randić	1.000	1.639	1.919	2.176	2.438	2.712	2.927	3.085	3.172
Ciesielski et. al.	2.000	2.185	1.919	1.740	1.625	1.550	1.464	1.371	1.269
Mandado	1.000	1.093	1.097	1.119	1.158	1.211	1.254	1.281	1.290
Two-term	2.000	1.355	1.029	0.844	0.727	0.648	0.592	0.551	0.508
Adjusted Two-term	2.000	0.892	0.648	0.504	0.426	0.350	0.307	0.277	0.254

Table 13: Scaling factors for linear polyacenes (L_∞).

Number of hexagons → Model ↓	1	2	3	4	5	6	7	8	9
Randić	1.000	1.639	2.169	2.176	2.438	2.712	2.516	2.684	2.867
Ciesielski et. al.	2.000	2.185	2.169	1.740	1.625	1.550	1.258	1.193	1.147
Mandado	1.000	1.093	1.183	1.119	1.158	1.211	1.117	1.148	1.186
Two-term	2.000	1.355	1.077	0.844	0.727	0.648	0.544	0.494	0.457
Adjusted Two-term	2.000	0.892	0.610	0.484	0.413	0.364	0.314	0.277	0.254

Table 14: Scaling factors for linear polyacenes (L_1).

Number of hexagons → Model ↓	1	2	3	4	5	6	7	8	9
Randić	1.000	1.639	1.894	2.151	2.255	2.340	2.385	2.411	2.428
Ciesielski et. al.	2.000	2.185	2.526	2.491	2.676	2.670	2.778	2.746	2.786
Mandado	1.000	1.093	1.003	1.006	0.927	0.927	0.910	0.907	0.900
Two-term	2.000	1.355	1.154	1.038	0.955	0.910	0.876	0.853	0.831
Adjusted Two-term	2.000	0.892	0.638	0.526	0.469	0.431	0.405	0.385	0.371

Table 15: Scaling factors for zigzag fibonacenes (L_∞).

Number of hexagons → Model ↓	1	2	3	4	5	6	7	8	9
Randić	1.000	1.639	1.894	2.151	2.255	2.679	2.706	2.754	2.769
Ciesielski et. al.	2.000	2.185	2.526	2.689	2.618	2.670	2.720	2.604	2.618
Mandado	1.000	1.093	1.003	1.006	0.954	0.936	0.930	0.861	0.856
Two-term Model	2.000	1.355	1.154	1.038	0.936	0.888	0.856	0.833	0.789
Adjusted Two-term Model	2.000	0.892	0.638	0.526	0.466	0.424	0.395	0.376	0.358

Table 16: Scaling factors for zigzag fibonacenes (L_1).

Number of hexagons → Model (Error) ↓	1	2	3	4	5	6	7	8	9
Randić ($L_\infty error$)	0.000	0.000	0.125	0.198	0.243	0.274	0.312	0.356	0.405
Ciesielski et. al. ($L_\infty error$)	0.000	0.000	0.125	0.198	0.243	0.274	0.312	0.356	0.405
Mandado ($L_\infty error$)	0.000	0.000	**0.079**	**0.136**	**0.174**	**0.201**	**0.231**	**0.268**	**0.309**
Two-term ($L_\infty error$)	0.000	0.000	**0.048**	0.096	0.138	0.173	0.201	0.223	0.260
Adjusted Two-term (L_∞)	0.000	0.000	0.068	**0.045**	**0.046**	**0.055**	**0.099**	**0.136**	**0.166**

Table 17: L_∞-errors for linear polyacenes.

Number of hexagons → Model (Error) ↓	1	2	3	4	5	6	7	8	9
Randić	0.000	0.000	0.999	2.373	3.599	5.253	7.093	8.556	10.470
Ciesielski et. al.	0.000	0.000	0.999	2.373	3.599	5.253	7.093	8.556	10.470
Mandado	0.000	0.000	**0.605**	**1.627**	**2.566**	**3.816**	**5.425**	**6.603**	**8.097**
Two-term	0.000	0.000	**0.359**	1.153	1.912	2.895	4.246	5.282	6.501
Adjusted Two-term	0.000	0.000	0.452	**0.532**	**0.309**	**0.798**	**1.458**	**2.060**	**2.600**

Table 18: L_1-errors for linear polyacenes.

Number of hexagons → Model (Error) ↓	1	2	3	4	5	6	7	8	9
Randić	**0.000**	0.000	0.217	0.146	0.190	0.177	0.184	0.181	0.182
Ciesielski et. al.	**0.000**	0.000	**0.035**	0.085	0.082	0.091	0.090	0.092	**0.091**
Mandado	**0.000**	0.000	0.039	**0.043**	**0.071**	**0.067**	**0.082**	**0.083**	**0.091**
Two-term	**0.000**	0.000	0.014	0.034	0.044	0.053	0.059	0.064	0.068
Adjusted Two-term	0.000	0.000	**0.012**	**0.017**	**0.014**	**0.020**	**0.033**	**0.042**	**0.049**

Table 19: L_∞-errors for zigzag fibonacenes.

Number of hexagons → Model ↓	1	2	3	4	5	6	7	8	9
Randić	0.000	0.000	1.303	1.457	2.500	2.584	2.982	3.019	3.267
Ciesielski et. al.	0.000	0.000	**0.213**	0.848	1.325	1.621	1.970	2.271	2.374
Mandado	0.000	0.000	0.233	**0.429**	**0.914**	**1.361**	**1.886**	**2.369**	**2.616**
Two-term ($L1error$)	0.000	0.000	0.083	0.345	0.657	0.888	1.155	1.420	1.567
Adjusted Two-term	0.000	0.000	**0.074**	**0.172**	**0.125**	**0.252**	**0.466**	**0.727**	**0.942**

Table 20: L_1-errors for zigzag fibonacenes.

5.1 The best matches to Hückel–London

Figures 28-31 gives the L_1- errors and L_∞- errors among all conjugated-circuit models as the number of hexagons increases for both linear polyacenes and zigzag fibonacenes except for one case that is shown in Section 5.1.1 where the Two-term model is best. The Adjusted Two-term model has minimum L_1 and L_∞-errors among all models discussed in this paper. Tables 19 and 20 show that Mandado has minimum L_1-error and L_∞-error as the number of hexagon increases for linear polyacenes. Tables 17 and 18 show, Mandado also gives minimum L_1-error and L_∞-error for zigzag fibonacenes as the number of hexagon increases, although there are cases when Ciesielski gives the minimum or equivalent L_1 or L_∞-errors. For the 3-hexagon zigzag fibonacene, Ciesielski gives minimum L_1 and L_∞-error and for the 9-hexagon zigzag fibonacene, Mandado and Ciesielski gave equivalent L_∞-error but Ciesielski gives minimum L_1-error.

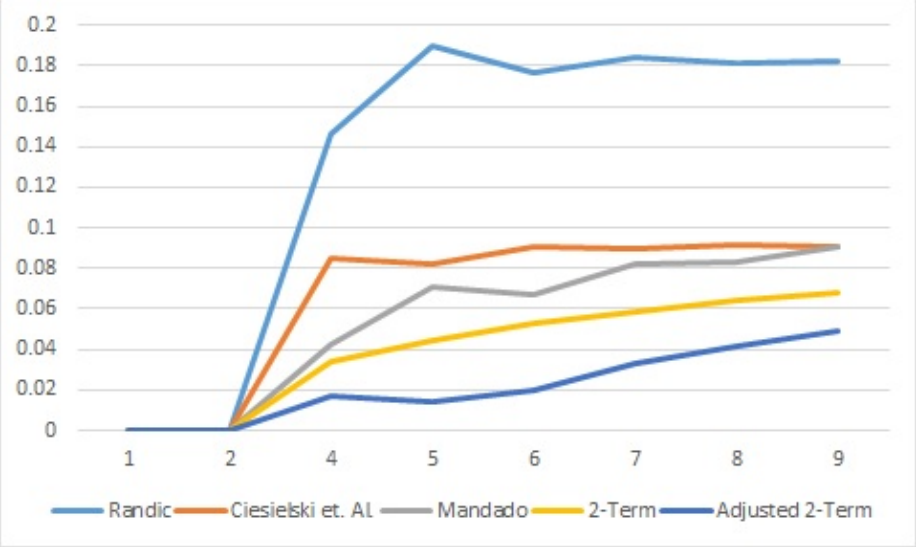

Figure 28: L_∞-error for zigzag fibonacenes.

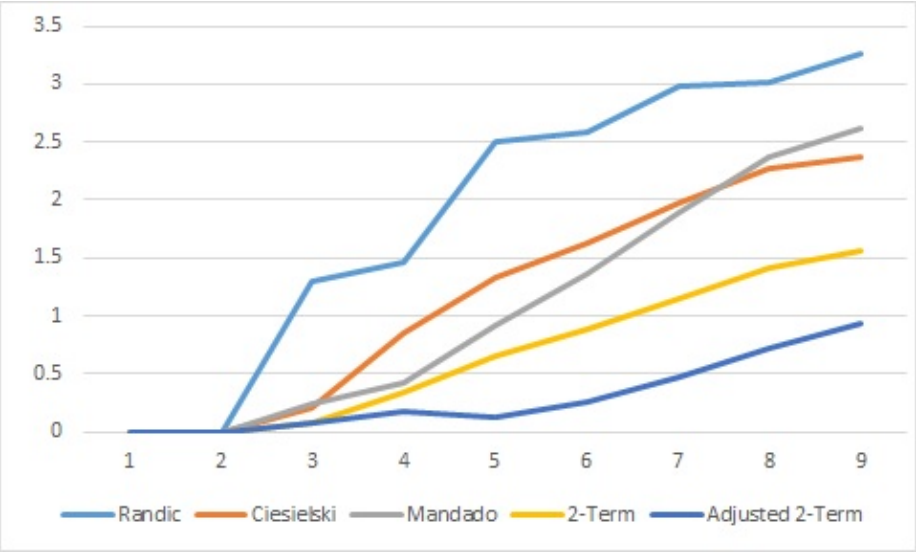

Figure 29: L_1-error for zigzag fibonacenes.

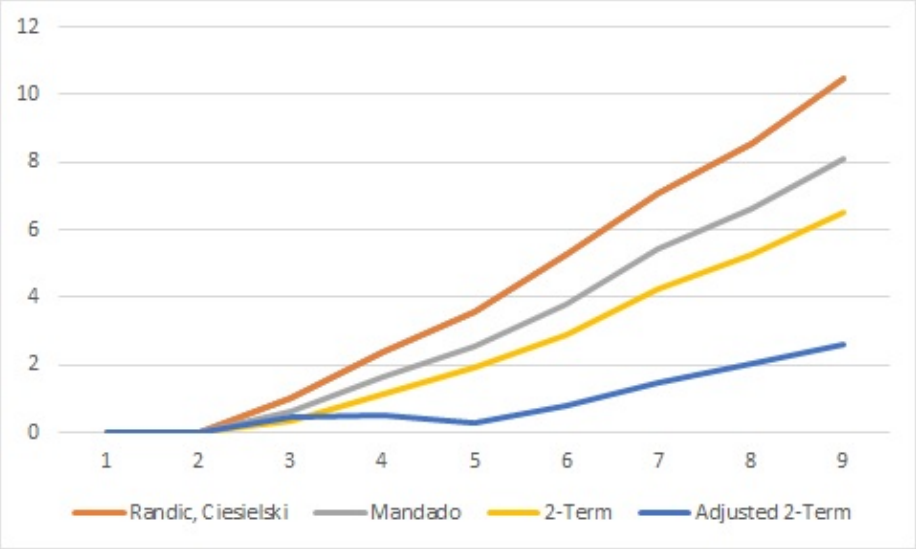

Figure 30: L_1-error for linear polyacenes.

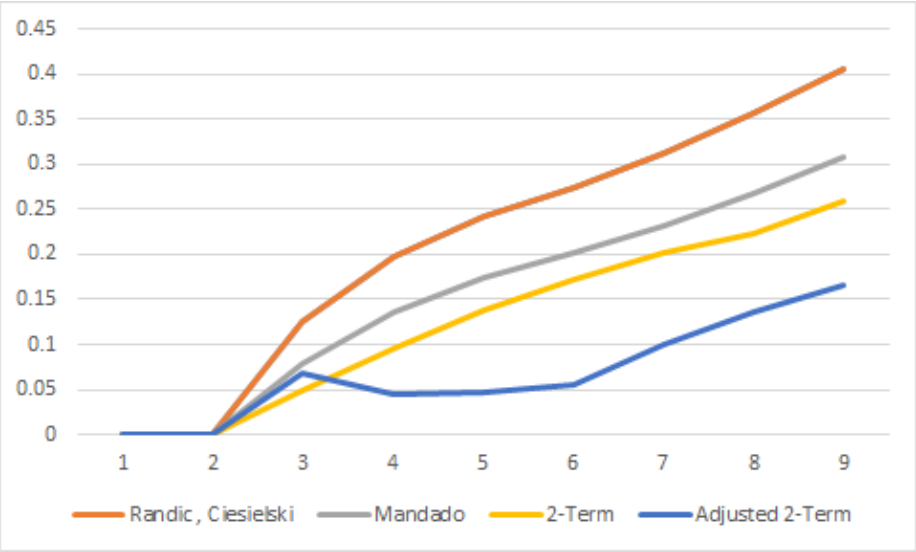

Figure 31: L_∞-error for linear polyacenes.

5.1.1 A case where the Two-term model gives less L_∞-error than the Adjusted Two-term model

For the 3-hexagon linear polyacenes, the Two-term model gives less L_∞-error than the Adjusted Two-term model as shown in Figure 33. Figure 32(a) shows the Hückel–London current, Figure 21 shows the Two-term current and Figure 22 shows the Adjusted Two-term current. The scaling factor for the Two-term model is 1.029 and the scaling factor for Adjusted Two-term model is 0.648. The difference in both models is the factor 4 in the Adjusted Two-term model. Possibly there is too much weight on the second term of the Two-term model for this case.

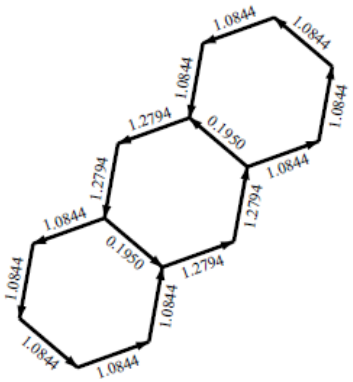

(a) Hückel–London currents.

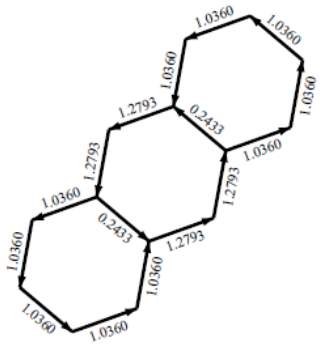

(b) The scaled Two-term current.

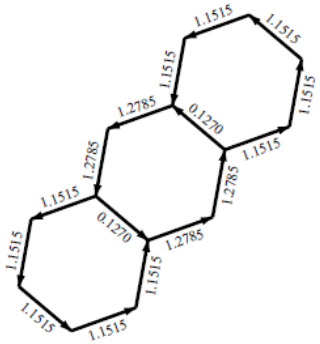

(c) The scaled Adjusted Two-term current.

Figure 32: Currents for 3-hexagon Linear Polyacene.

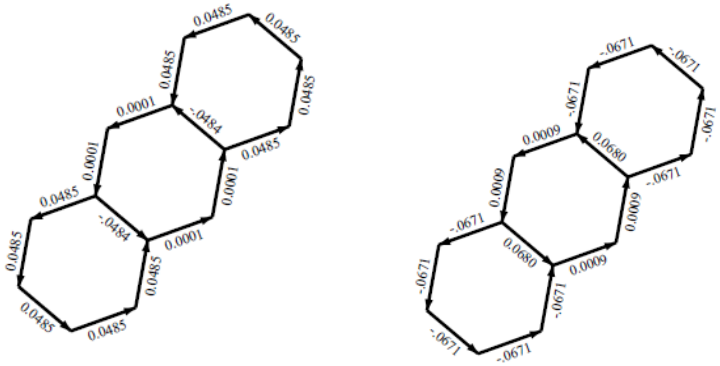

(a) The $L_\infty - error$ for Two-term current model.

(b) The $L_\infty - error$ for Adjusted Two-term current model.

Figure 33: The Two-term model gives a smaller L_∞-error than the Adjusted Two-term model for 3-hexagon Linear Polyacene.

6 Conclusions and Future work

This paper work shows results which are computed using a set of software. For existing conjugated-circuit models currents were computed using Bill Bird's project software [3]. Myrvold and Fowler provided their computations for the new models [11]. The Simplex method, generation of the benzenoid families, formulation of Linear Programming problems for families, scaled currents, errors between current models were programmed by the author and the linking of tasks was automated. The scaling factors and errors were checked independently by Myrvold. These results can be verified using SCIP [7] for future work.

The results shows that the Adjusted Two-term model gives better approximations to the Hückel–London model except for the one case discussed in Section 5.1.1. It is still debatable if the Two-term should be adjusted with a different value, possibly dependent on on some variable n or $m(G)$. Do these models show consistent patterns of internal or external ring currents? Do they show common high or low currents in a certain pattern? Also, It is hard to say

from this research which error measure is better L_1-error or L_∞- error as the model which gave the best or the worst results in L_1 approach was the same for the L_∞.

References

[1] Aihara. *J. Journal of the American Chemical Society*, 101:558, 1979.

[2] Aihara. *J. Journal of the American Chemical Society*, 101:5913, 1979.

[3] Bill Bird. Comparison of combinatorial models for ring currents. *Honours Project, University of Victoria*, pages 1–24, 2011.

[4] Vašek Chvátal. *Linear programming*. W.H. Freeman, New York, 1983.

[5] Arkadiusz Ciesielski, Tadeusz M. Krygowski, Michał K. Cyrański, Michał A. Dobrowolski, and Jun-ichi Aihara. Graph-topological approach to magnetic properties of benzenoid hydrocarbons. *Physical chemistry chemical physics : PCCP*, 11(48):11447, 2009.

[6] Patrick W. Fowler and Wendy Myrvold. The "anthracene problem": closed-form conjugated-circuit models of ring currents in linear polyacenes. *The journal of physical chemistry. A*, 115(45):13191–13200, 2011.

[7] Gerald Gamrath, Tobias Fischer, Tristan Gally, Ambros M. Gleixner, Gregor Hendel, Thorsten Koch, Stephen J. Maher, Matthias Miltenberger, Benjamin Müller, Marc E. Pfetsch, Christian Puchert, Daniel Rehfeldt, Sebastian Schenker, Robert Schwarz, Felipe Serrano, Yuji Shinano, Stefan Vigerske, Dieter Weninger, Michael Winkler, Jonas T. Witt, and Jakob Witzig. The scip optimization suite 3.2. Technical Report 15-60, ZIB, Takustr.7, 14195 Berlin, 2016.

[8] Horikawa J., Aihara. *T. Bulletin of the Chemical Society of Japan*, 56:1853, 1983.

[9] Marcos Mandado. Determination of London Susceptibilities and Ring Current Intensities using Conjugated Circuits. *Journal of chemical theory and computation*, 5(10):2694–2701, 2009.

[10] Gerard Meurant. *Computer Solution of Large Linear Systems*. 1999.

[11] Myrvold and Fowler. Personal Communication. 2017.

[12] Randić. Graph theoretical approach to π-electron currents in polycyclic conjugated hydrocarbons. *Chemical Physics Letters*, 115(1-3):13191–13200, 2011.

[13] Lionel Salem. *The molecular orbital theory of conjugated systems*. W.A. Benjamin, Reading, Mass, 1974.

[14] Douglas B. West. *Introduction to graph theory*. Prentice Hall, Upper Saddle River, NJ, 1996.